Stability of normal mode oscillations of one-dimensional anharmonic lattices

K. Yoshimura
Department of Applied Mathematics and Physics, Kyoto University, Kyoto 606-01, Japan
(Received 30 April 1996)

The stability of motions in short periods of time has been investigated under the single-mode excitation condition for the Fermi-Pasta-Ulam-β model. It is the main concern of this paper to determine the stability against both the energy density and the excited mode's wave number. We propose the average variational equation as a tool for the stability analysis. The stability is also examined by the numerical integration of the equations of motion and the results are in good agreement with those of the theoretical analysis. We show that the stability is intricately dependent on the energy density and the excited mode's wave number. In particular, it is found that the motion of the normal mode whose wave number is within a specific range is extremely stable. [S1063-651X(96)03311-9]

PACS number(s): 46.10.+z, 05.45.+b, 05.20.−y

I. INTRODUCTION

The study of the stability properties of motions of one-dimensional anharmonic lattices started by Fermi, Pasta, and Ulam [1] was concerned with the dynamical foundations of classical statistical mechanics. It is well known that the observed motions were not stochastic but rather regular, contrary to their expectation: instead of the stochastic energy exchange among the normal modes, an almost periodic and regular energy exchange was observed. After Fermi, Pasta, and Ulam's work, the stability properties of one-dimensional anharmonic lattices and their relation to the ergodic properties were of great interest, and many studies have been done on the problem [2–16].

To study the stability properties of one-dimensional anharmonic lattices, the simplest problem is that of the single-mode excitation or the narrow packet excitation: only one normal mode with a wave number k is initially excited or a wave packet with mean wave number k and small size $\delta k/k \ll 1$, where δk is the characteristic size of the packet in k space, is initially excited. This simple problem is important to understand the dynamics of one-dimensional anharmonic lattices. However, it has not been fully understood in spite of its importance. We will study this problem in the present paper.

There are some analytical and numerical results concerning the problem. It has been found by works following [1] that there is a certain kind of the stochasticity limit, which is defined as the critical energy density (energy per degree of freedom) distinguishing the stable and stochastic motions. First, we speak of analytical results that determine the stochasticity limit against the number of degrees of freedom, and the wave number of the excited mode. For the Fermi-Pasta-Ulam (FPU) β model, one of the most widely known analytical results is that of Izrailev and Chirikov obtained by applying the resonance overlap criterion [3] (see also Ref. [17]). The resonance overlap criterion had been developed as the method determining the stochasticity limit of a Hamiltonian system with small degrees of freedom. In order to apply the criterion to the FPU-β model with large degrees of freedom, Izrailev and Chirikov reduced the dimensionality of the system in a way that could permit the application of the resonance overlap criterion, taking into account only one of the resonance terms. Applying the resonance overlap criterion, the stochasticity limit ϵ_c was determined as

$$\epsilon_c \sim \begin{cases} \dfrac{1}{\beta k}, & k \ll N \\ \dfrac{\pi^2 k^2}{\beta N^4}, & N-k \ll N, \end{cases} \tag{1}$$

where β is the nonlinear coupling constant, k the wave number of the excited mode, and N the number of degrees of freedom. The stochastic motions appear in the energy density range $\epsilon > \epsilon_c$. Generally speaking, if the mode with the larger wave number k is more stochastic at a fixed energy density, the ϵ_c should decrease with an increase in the k correspondingly. Hence the result of the case of $k \ll N$ in Eq. (1) indicates that the larger-wave-number mode excitation is more stochastic. In view of this fact, the lack of the stochasticity observed in Ref. [1] was attributed to the smallness of the wave number chosen in Fermi-Pasta-Ulam's numerical experiments. On the other hand, Berman and Kolovskij approximated the FPU-β model by the nonlinear Schrödinger equation under the narrow packet condition $\delta k/k \ll 1$ to determine the stochasticity limit [4]. The stochasticity limit was obtained as

$$\epsilon_c \sim \frac{2\pi^2 k}{3\beta N^2}. \tag{2}$$

This indicates that the larger-wave-number mode excitation is less stochastic and qualitatively agrees with the result of the case of $N-k \ll N$ in Eq. (1). These two analytical results are necessarily qualitative and perhaps, in our opinion, fail to grip the whole picture of the stability properties because the drastic simplifications are introduced in the analyses.

Regarding the numerical results, the situation is still ambiguous and there is no definitive result to the problem. Here we refer to the results for the FPU-β model presented in Ref. [12]. In that paper the authors defined the relaxation time as the time needed for energy concentrated on a narrow packet

at the initial to be distributed over most of the modes. The longer relaxation time can be reasonably considered to mean less efficient stochastic pumping in phase space. Therefore, they numerically computed the relaxation time as a measure of the stochasticity. The observed relaxation time has the tendency, roughly speaking, to increase with increasing the wave number when the energy density is smaller than a certain critical value, while the opposite tendency is observed for the energy density larger than the critical value (in Ref. [12], Fig. 11). Their main consequence is that the stochasticity has the opposite dependence on the wave number between the lower- and higher-energy density range.

The stability properties of the single-mode excitation or the narrow packet excitation have not been fully understood, in spite of their importance in understanding the dynamics of one-dimensional anharmonic lattices. In fact, the results are different among the above-mentioned works. The present paper aims to clarify, for the specific case of the FPU-β model, how the stability depends on the energy density and the wave number when a single normal mode is initially excited. We conjecture that the stability is more intricately dependent on the wave number and on the energy density, contrary to the simple dependences stated in the above-mentioned works. Our results support the conjecture; the stochasticity of the normal mode is enhanced intermittently in some specific ranges of the wave number, while the normal modes having the wave number within a certain range are extremely stable. These findings are quite recent and have not yet been reported elsewhere to our knowledge.

For the above-mentioned purpose, we propose a kind of average variational equation as a tool to examine the stability of the normal mode and numerically solve the equation. To make a comparison, we numerically integrate the equations of motion of the relevant model, computing the relaxation time to quantify the stability. The present paper is organized as follows. In Sec. II, we describe the FPU-β model, the average variational equation, and the relaxation time. In Sec. III, we report the results of the numerical calculations and give the discussion. In Sec. IV, some conclusions are drawn.

II. DYNAMICAL MODEL AND TOOLS OF STABILITY ANALYSIS

A. FPU-β model and stability of the normal mode

In the present paper, our investigation is made for the dynamical model described by the Hamiltonian

$$H=\frac{1}{2}\sum_{i=1}^{N-1} p_i^2+\sum_{i=1}^{N}\left[\frac{1}{2}(q_i-q_{i-1})^2+\frac{\beta}{4}(q_i-q_{i-1})^4\right], \tag{3}$$

which is called the FPU-β model. This Hamiltonian describes the one-dimensional anharmonic lattice with nearest-neighbor interaction. We set $\beta=1$ and $N=128$. As the boundary condition we employ the fixed-end condition, i.e.,

$$q_0=q_N=0. \tag{4}$$

The equations of motion derived from the Hamiltonian are

$$\frac{d^2q_i}{dt^2}=q_{i+1}+q_{i-1}-2q_i+\beta\{(q_{i+1}-q_i)^3-(q_i-q_{i-1})^3\}. \tag{5}$$

For convenience of discussion, we introduce the normal mode coordinates. The transformation $\mathbf{q}\mapsto\mathbf{Q}$ defined by

$$q_i=\sqrt{\frac{2}{N}}\sum_{k=1}^{N-1} Q_k\sin\left(\frac{\pi k}{N}i\right) \quad (i=1,2,\ldots,N-1) \tag{6}$$

gives the normal modes of the corresponding harmonic system. Q_k is the amplitude of the kth normal mode. The characteristic frequency of the kth normal mode is given as

$$\omega_k=2\sin\left(\frac{\pi k}{2N}\right). \tag{7}$$

In terms of the normal modes coordinates $\mathbf{Q}$ and the conjugate momenta $\mathbf{P}$, the Hamiltonian is rewritten as

$$\begin{aligned}H=&\sum_{k=1}^{N-1}\left(\frac{1}{2}P_k^2+\frac{1}{2}\omega_k^2Q_k^2\right)\\&+\frac{\beta}{8N}\sum_{k_1,k_2,k_3,k_4=1}^{N-1}\omega_{k_1}\cdots\omega_{k_4}Q_{k_1}\cdots Q_{k_4}\\&\times D(k_1,k_2,k_3,k_4),\end{aligned} \tag{8}$$

where $D(k_1,k_2,k_3,k_4)$ represents the selection rule of the interaction among the normal modes and it is explicitly written as

$$\begin{aligned}D(k_1,k_2,k_3,k_4)=&\delta(k_1+k_2,k_3+k_4)+\delta(k_1+k_3,k_2+k_4)\\&+\delta(k_1+k_4,k_2+k_3)+\delta(k_1+k_2+k_3,k_4)\\&+\delta(k_1+k_2+k_4,k_3)+\delta(k_1+k_3+k_4,k_2)\\&+\delta(k_2+k_3+k_4,k_1)-\delta(k_1+k_2+k_3\\&+k_4,2N)-\delta(k_1+k_2+k_3,2N+k_4)\\&-\delta(k_1+k_2+k_4,2N+k_3)\\&-\delta(k_1+k_3+k_4,2N+k_2)\\&-\delta(k_2+k_3+k_4,2N+k_1),\end{aligned} \tag{9}$$

where δ is the Kronecker delta function. The equation of motion for the kth normal mode is

$$\begin{aligned}&\frac{d^2}{dt^2}Q_k+\omega_k^2Q_k+\frac{\beta}{2N}\\&\quad\times\sum_{k_1,k_2,k_3=1}^{N-1}\omega_k\omega_{k_1}\omega_{k_2}\omega_{k_3}Q_{k_1}Q_{k_2}Q_{k_3}D(k,k_1,k_2,k_3)\\&=0.\end{aligned} \tag{10}$$

As the stability of the normal mode is the main subject of the present study, one must be clear about the definition of the stability. We mention the definition in the following. The initial condition discussed in the present study is the single-

mode excitation condition; when the kth normal mode is excited, the amplitudes of the other modes are set to zero at the initial condition

$$Q_i(0)=\dot{Q}_i(0)=0 (i\neq k). \tag{11}$$

Due to this initial condition, $Q_i(t)\simeq 0 (i\neq k)$ holds for a short period of time $t<\tau_s$. τ_s is the time scale within which the single-mode oscillation of the kth mode lasts without significant energy exchange with the other modes. The time scale τ_s depends on the wave number k and the energy density ϵ, where ϵ is related to the total energy E as $\epsilon=E/N$. We define the stability of the normal mode in terms of the τ_s; if τ_s is large, the normal mode is regarded as stable. The method of estimating τ_s by the numerical experiments will be described.

If the approximation $Q_i(t)\simeq 0 (i\neq k)$ is made in Eq. (10), the equation of motion for the kth normal mode, which is the mode excited initially, is approximated as

$$\frac{d^2}{dt^2}Q_k+\omega_k^2 Q_k+\frac{3\beta}{2N}\omega_k^4 Q_k^3=0. \tag{12}$$

It is well known that the solution of Eq. (12) may be written, with the Jacobi elliptic function, in the form

$$\tilde{Q}_k(t)=\sqrt{N}a\ \mathrm{cn}(\sigma t,k'^2), \tag{13}$$

where

$$a^2=\frac{4k'^2}{3\beta\omega_k^2(1-2k'^2)},\quad \sigma^2=\frac{\omega_k^2}{1-2k'^2}, \tag{14}$$

and k'^2 is the modulus of the Jacobi elliptic function. The modulus k'^2 is related to the energy density ϵ as

$$\epsilon=\frac{2k'^2(1-k'^2)}{3\beta(1-2k'^2)^2}. \tag{15}$$

In phase space, the motion associated with $\tilde{Q}_k(t)$ forms the periodic orbit $\tilde{\mathbf{\Gamma}}(t)=(\tilde{\mathbf{q}}(t),\tilde{\mathbf{p}}(t))$, where $\tilde{\mathbf{q}}=(\tilde{q}_1,\ldots,\tilde{q}_{N-1})$ is the positions obtained through the transformation Eq. (6) as

$$\tilde{q}_i=\sqrt{\frac{2}{N}}\,\tilde{Q}_k\sin\left(\frac{\pi k}{N}i\right)\quad (i=1,2,\ldots,N-1), \tag{16}$$

and $\tilde{\mathbf{p}}=(\tilde{p}_1,\ldots,\tilde{p}_{N-1})$ are the conjugate momenta. Since $\tilde{Q}_k(t)$ is not the exact solution but the approximate one, the periodic orbit $\tilde{\mathbf{\Gamma}}(t)$ is also the approximate one. In this sense, we call $\tilde{\mathbf{\Gamma}}(t)$ the *pseudoperiodic orbit*. An orbit starting with the single-mode excitation condition may stay close to the pseudoperiodic orbit during a certain short period, and then it may diffuse in phase space. The length of the period is characterized by τ_s. That is, τ_s is the time scale of the diffusion in phase space.

B. Average variational equation

In this subsection, we describe the *average variational equation*, which we propose as a tool to examine the stability of the normal mode. Let us consider a generic Hamiltonian system of the form

$$H=\sum_{i=1}^{n}\frac{p_i^2}{2}+V(\mathbf{q}), \tag{17}$$

where $V(\mathbf{q})$ is a nonlinear interaction potential among n particles with unit mass, positions $\mathbf{q}=(q_1,\ldots,q_n)$, and momenta $\mathbf{p}=(p_1,\ldots,p_n)$. The FPU-$\beta$ model is also included in this class. The equations of motion derived from the Hamiltonian

$$\frac{dq_i}{dt}=p_i,\quad \frac{dp_i}{dt}=-\frac{\partial V}{\partial q_i}\quad (i=1,2,\ldots,n), \tag{18}$$

exhibit the stochastic motions for most of the interesting choices of $V(\mathbf{q})$. One of the characteristic features of the stochastic motions is exponential growth of distance between nearby orbits in phase space. Hence the stochasticity of motions can be quantified by the rates of the exponential growth.

The exponential growth of distance is usually examined through the variational equation, which is obtained by linearizing the equations of motion (18) along a reference orbit $(\mathbf{q}(t),\mathbf{p}(t))$. Let $\delta\mathbf{q}=(\delta q_1,\ldots,\delta q_n)$ and $\delta\mathbf{p}=(\delta p_1,\ldots,\delta p_n)$ be the variations of the coordinates and the momenta, respectively. The variational equation is given in the form

$$\frac{d\boldsymbol{\xi}}{dt}=\underline{A}(\mathbf{q}(t))\boldsymbol{\xi} \tag{19}$$

for variations $\boldsymbol{\xi}=(\delta\mathbf{q},\delta\mathbf{p})$. The $2n\times 2n$ matrix $\underline{A}(\mathbf{q}(t))$ is defined as

$$\underline{A}(\mathbf{q}(t))=\begin{pmatrix}\underline{0} & \underline{I}\\ -\underline{V}(\mathbf{q}(t)) & \underline{0}\end{pmatrix}, \tag{20}$$

where 0 and I are the $n\times n$ null and unit matrices, respectively, and $\underline{V}(\mathbf{q}(t))$ is the $n\times n$ matrix of second derivatives of V whose elements are defined as

$$[\underline{V}(\mathbf{q}(t))]_{ij}=\frac{\partial^2 V(\mathbf{q}(t))}{\partial q_i\partial q_j}. \tag{21}$$

The solution $\boldsymbol{\xi}(t)$ of Eq. (19) grows exponentially when the exponential divergence of nearby orbits of the original dynamical system Eq. (18) occurs.

The stability of the normal mode, which has been defined in terms of the τ_s, can be reasonably considered to be quantified also in terms of the exponential growth rates: the smaller τ_s corresponds to the larger exponential growth rates. As we are interested in the short-time stability of the normal mode, the exponential growth rates of the short period of time $t<\tau_s$ are useful. Based on the fact that any orbits starting with the single mode excitation condition stay close to the pseudoperiodic orbit for $t<\tau_s$, we employ the varia-

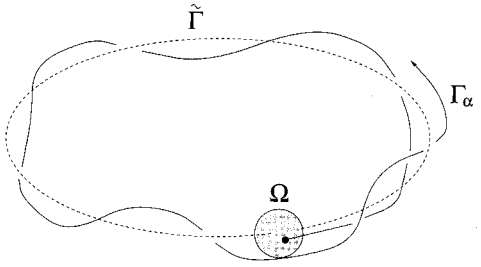

FIG. 1. Schematic illustration for a pseudoperiodic orbit.

tional equation along the pseudoperiodic orbit to obtain the approximate exponential growth rates of the short period of time. That is, the variational equation employed is

$$\frac{d\boldsymbol{\xi}}{dt}=\underline{A}(\tilde{\mathbf{q}}(t))\boldsymbol{\xi}, \tag{22}$$

where $\tilde{\mathbf{q}}(t)$ is the positions defined by Eq. (16). For the FPU-β model with the fixed ends, the $(N-1)\times(N-1)$ elements of second derivatives of V, which are included in the matrix $\underline{A}$, are written as

$$\frac{\partial^2 V}{\partial q_i \partial q_j}=\begin{cases} 2+3\beta\{(q_i-q_{i+1})^2+(q_i-q_{i-1})^2\}, & i=j \\ -1-3\beta(q_i-q_j)^2, & i=j\pm 1 \\ 0 \quad \text{otherwise.} \end{cases} \tag{23}$$

We make mention of the solution of Eq. (22). Since the $\tilde{\mathbf{q}}(t)$ is periodic, the matrix $\underline{A}(\tilde{\mathbf{q}}(t))$ is also periodic. According to the Floquet theory, the solution can be obtained in the form

$$\underline{\Phi}(t)=\underline{P}(t)\exp(t\underline{\Lambda}), \tag{24}$$

where $\Phi(t)$ is the $(N-1)\times(N-1)$ matrix whose columns consist of the independent solutions of Eq. (22), $P(t)$ the $(N-1)\times(N-1)$ matrix whose elements are periodic functions with the same period as $\underline{A}(\tilde{\mathbf{q}}(t))$, and Λ the $(N-1)\times(N-1)$ constant matrix. It depends on real parts of eigenvalues of the matrix Λ whether or not the solution of Eq. (22) is unstable (exponentially growing): if there are eigenvalues of the positive real part, the solution is unstable. The largest real part λ_1, which is called the *largest characteristic exponent* (LCE), gives the maximum growth rate of the solution, and it is useful to quantify the stability of the normal mode. The λ_1 is calculated to quantify the stability.

At the end of this subsection, we mention the reason why we call Eq. (22) the average variational equation. We take the pseudoperiodic orbit $\tilde{\boldsymbol{\Gamma}}(t)=(\tilde{\mathbf{q}}(t),\tilde{\mathbf{p}}(t))$ in phase space. A schematic illustration of phase space is shown in Fig. 1. Let Ω be a certain small ensemble of initial phase points near the point $\tilde{\boldsymbol{\Gamma}}(0)=(\tilde{\mathbf{q}}(0),\tilde{\mathbf{p}}(0))$ and $\boldsymbol{\Gamma}_\alpha(t)$ be a solution of Eq. (18), which has the initial point $\boldsymbol{\Gamma}_\alpha(0)$ within the Ω. The variational equation along $\boldsymbol{\Gamma}_\alpha(t)$ is

$$\frac{d}{dt}\boldsymbol{\xi}(t;\boldsymbol{\xi}_0)=\underline{A}(\boldsymbol{\Gamma}_\alpha(t))\boldsymbol{\xi}(t;\boldsymbol{\xi}_0), \tag{25}$$

where $\boldsymbol{\xi}(t;\boldsymbol{\xi}_0)$ is the solution that satisfies $\boldsymbol{\xi}(0;\boldsymbol{\xi}_0)=\boldsymbol{\xi}_0$ and $A(\boldsymbol{\Gamma}_\alpha(t))$ stands for $A(\mathbf{q}_\alpha(t))$. If we take the ensemble average in Eq. (25) over the Ω, we obtain the equation

$$\frac{d}{dt}\langle\boldsymbol{\xi}(t;\boldsymbol{\xi}_0)\rangle=\langle\underline{A}(\boldsymbol{\Gamma}_\alpha(t))\boldsymbol{\xi}(t;\boldsymbol{\xi}_0)\rangle, \tag{26}$$

where $\langle\rangle$ represents the ensemble average with respect to the initial phase points $\boldsymbol{\Gamma}_\alpha(0)$ over the Ω. We divide $\boldsymbol{\xi}(t;\boldsymbol{\xi}_0)$ into the average and the deviation from it,

$$\boldsymbol{\xi}(t;\boldsymbol{\xi}_0)=\langle\boldsymbol{\xi}(t;\boldsymbol{\xi}_0)\rangle+\delta\boldsymbol{\xi}(t), \tag{27}$$

and substitute into Eq. (26). Then, we obtain

$$\frac{d}{dt}\langle\boldsymbol{\xi}(t;\boldsymbol{\xi}_0)\rangle=\langle\underline{A}(\boldsymbol{\Gamma}_\alpha(t))\rangle\langle\boldsymbol{\xi}(t;\boldsymbol{\xi}_0)\rangle+\langle\underline{A}(\boldsymbol{\Gamma}_\alpha(t))\delta\boldsymbol{\xi}(t)\rangle. \tag{28}$$

Since the ensemble Ω is sufficiently small and close to the point $\tilde{\boldsymbol{\Gamma}}(0)$, it can be expected that, for the short period of time $t<\tau_s$, the sample orbits $\boldsymbol{\Gamma}_\alpha(t)$ stay close to the pseudo periodic orbit $\tilde{\boldsymbol{\Gamma}}(t)$. Hence we assume that the second term that contains $\delta\boldsymbol{\xi}(t)$ on right-hand side of Eq. (28) can be neglected and $\langle\underline{A}(\boldsymbol{\Gamma}_\alpha(t))\rangle\simeq\underline{A}(\tilde{\boldsymbol{\Gamma}}(t))$. If we admit the assumption, then we obtain

$$\frac{d}{dt}\langle\boldsymbol{\xi}(t;\boldsymbol{\xi}_0)\rangle=\underline{A}(\tilde{\boldsymbol{\Gamma}}(t))\langle\boldsymbol{\xi}(t;\boldsymbol{\xi}_0)\rangle. \tag{29}$$

This equation describes, for the short period of time, the time evolution of the ensemble average of the variation $\boldsymbol{\xi}$. Equation (29) is just the same as Eq. (22). Therefore, Eq. (22) can be interpreted as the variational equation, which describes the time evolution of the ensemble average of $\boldsymbol{\xi}$. In this sense, we call Eq. (22) the average variational equation. The LCE has the local meaning in phase space, that is, it represents the mean divergence rate between nearby orbits in the vicinity of the pseudoperiodic orbit.

C. Relaxation time

The time scale τ_s is estimated by the numerical integration of the equations of motion (5) to examine the stability of the normal mode. In this subsection, we describe how we estimate τ_s.

We define the harmonic energy E_i of each normal mode as

$$E_i(t)=\frac{1}{2}[\dot{Q}_i^2(t)+\omega_i^2 Q_i^2(t)] \tag{30}$$

and the weights w_i, which give the fraction of the total harmonic energy in each normal mode, by

$$w_i(t)=\frac{E_i(t)}{\sum_{m=1}^{N-1}E_m(t)}. \tag{31}$$

Let us define the spectral entropy $S(t)$ as [11]

$$S(t)=\sum_{i=1}^{N-1} -w_i(t)\ln w_i(t). \tag{32}$$

$S(t)$ can be normalized as

$$\eta(t)=\frac{S_{\max}-S(t)}{S_{\max}-S(0)}, \tag{33}$$

where $S_{\max}=\ln(N-1)$. $\eta(t)$ is a parameter to measure the extent of the energy exchange among the normal modes. If there is no energy exchange among the normal modes $S(t)=S(0)$, $\eta(t)$ remains unity. On the contrary, $\eta(t)$ decreases if the energy exchange occurs; $\eta(t)=0$ represents the state where energy is equally shared among all the normal modes. We define the relaxation time τ_R as the time at which $\eta(t)$ reaches 0.6, i.e., $\eta(\tau_R)=0.6$. The time scale τ_s can be estimated by calculating the relaxation time τ_R defined above. We will use the inverse of the relaxation time $1/\tau_R$ as a stochasticity indicator, which can be considered proportional to the stochasticity of the normal mode.

III. RESULTS AND DISCUSSION

It has been studied via the average variational equation how the stability of the normal mode varies with the wave number k and the energy density ϵ. We have numerically calculated the LCE of the average variational equation (22) for various sets of k and ϵ. The results are shown in Fig. 2, where the LCE is plotted as a function of the relative wave number k/N and the energy density ϵ, i.e., $\lambda_1(k/N,\epsilon)$. $\lambda_1(k/N,\epsilon)$ is represented in Fig. 2(a), and the contour plot is in Fig. 2(b).

The qualitatively different new features can be found in Fig. 2, in addition to the expected tendency that λ_1 increases with increasing energy density at a fixed wave number. That is, there is the interval in the wave number in which λ_1 shows a sharp decrease and remains remarkably small even at the large energy density. The interval is located at $k/N\simeq 0.7$. This predicts that if the normal mode having the wave number within the interval is excited, it oscillates for a long time without significant energy exchange with the other normal modes, namely, τ_s (or τ_R) of the mode is large. As the normal mode in the interval is stable, we call the interval in k space the *stability band*. The other feature is that there are some peaks of λ_1 in the relative wave-number range smaller than that of the stability band. Three peaks of the λ_1 can be clearly seen at $k/N\simeq$ 0.50, 0.34, and 0.24 and more peaks, which are very weak, may be perceivable in the smaller wave number range. The existence of these peaks predicts that the stochasticity is enhanced intermittently at some specific values of the k/N corresponding to the peaks. We call this feature the *ridge structure*.

It is seen in Fig. 2 that λ_1 tends to increase as k/N increases at a fixed energy density if one ignores the above-mentioned peaks of λ_1. This means that the mode of the larger wave number tends to be more stochastic. Correspondingly, the energy density ϵ_c' at which λ_1 has a certain constant value, namely, one of the contour curves, is lowered with increasing wave number. Approximately, the following relation can be found from the figure:

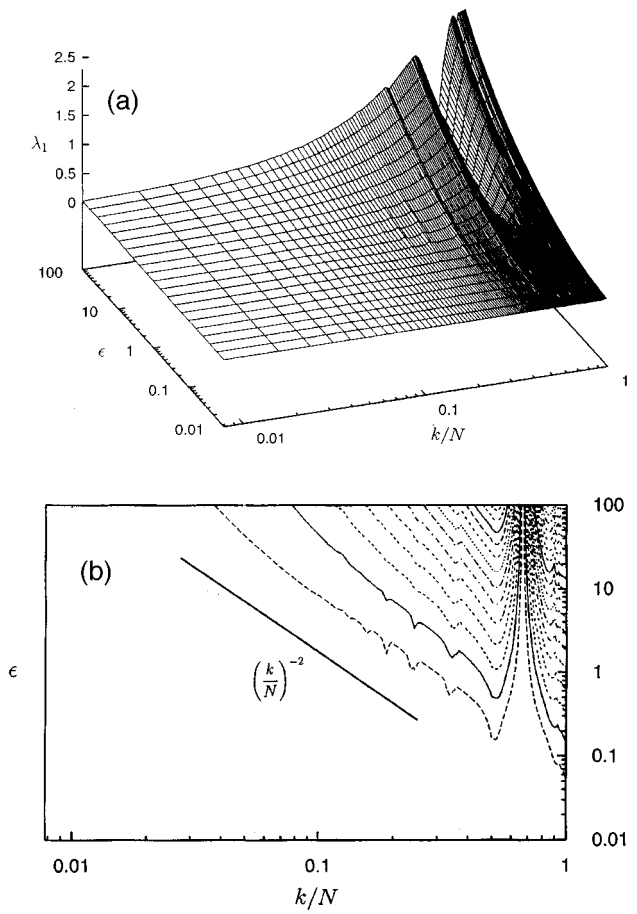

FIG. 2. (a) LCE λ_1 plotted as a function of ϵ and k/N. (b) Contour plot. The reference line of the power law $(k/N)^{-2}$ is also plotted.

$$\epsilon_c'\sim\left(\frac{k}{N}\right)^{-2}. \tag{34}$$

This relation between ϵ_c' and the k is in agreement qualitatively with that of the ϵ_c obtained by Izrailev and Chirikov in Ref. [3] [see Eq. (1)]: both ϵ_c and the ϵ_c' become lower with increasing k, although they are quantitatively different with respect to the exponents of the power laws. Therefore, ϵ_c' can be considered similar to ϵ_c.

We proceed to the numerical experiments to confirm the above predictions made by the LCE analysis. The relaxation time τ_R has been calculated for various sets of k/N and ϵ to make a comparison with the results of the LCE. The numerical integration of the equations of motion has been performed by the leapfrog algorithm because of its symplectic nature and simplicity.

τ_R has been calculated only for odd wave number k for the following reason. If one normal mode is excited initially, the normal modes allowed to be excited are restricted due to the selection rule $D(k_1,k_2,k_3,k_4)$: for instance, in the case of $N=128$, (i) if the mode of $k=4$ is excited initially, $k=4,12,20,28,36,44,52,60,68,76,84,92,100,108,116,$ and 124 are allowed; (ii) if $k=16$ is excited initially, $k=16,48,80,$ and 112 are allowed; and (iii) if $k=64$ is excited initially, no other modes can be excited. A detailed discussion on the mode selection has been given in Ref. [6].

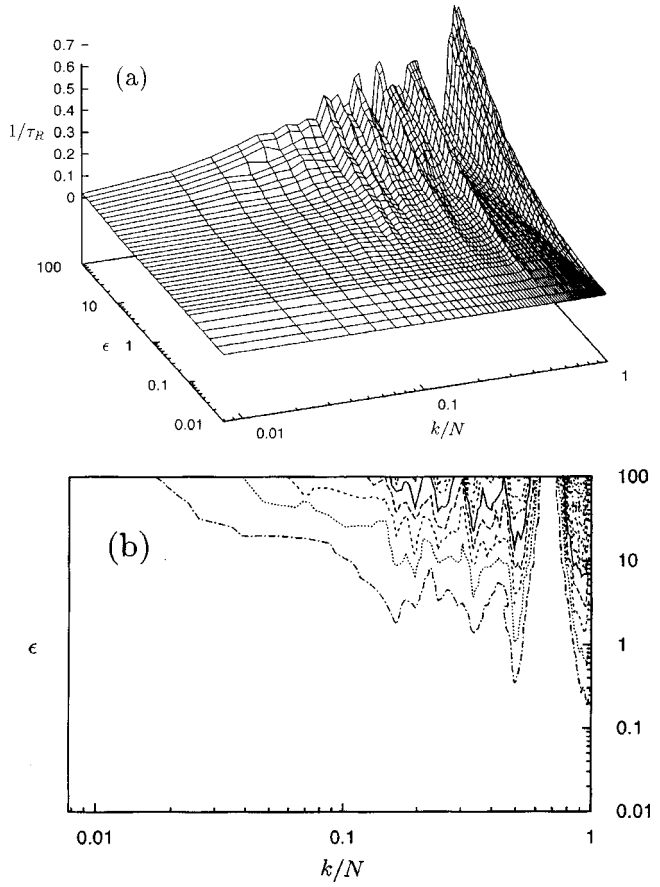

FIG. 3. (a) Inverse of the relaxation time $1/\tau_R$ plotted as a function of ϵ and k/N. (b) Contour plot.

As seen in the examples, when the mode of even wave number is excited initially, the number of allowed modes is considerably different, according to the initial-excited wave number. This difference has a significant effect on the decay of $\eta(t)$ and thus on τ_R, especially in the case that only a small number of the modes are allowed. The $\eta(t)$ cannot reach the reference value of 0.6 when only a few modes are allowed: for instance, as only four modes are allowed in the case of $k=16$ excitation, $\eta(t)$ cannot decrease less than $1-\ln 4/\ln 128$ ($\simeq 0.714$), which corresponds to the case that energy is equally shared among the four allowed modes. In such a case, τ_R cannot be used as a stochasticity indicator. In contrast, in the case of $N=128$, if the mode of odd wave number is excited initially, all the modes of odd wave number are always allowed. Then, there is no difference in the number of allowed modes. This is the reason why we have made the calculation of τ_R only for odd wave number.

We briefly comment on the reliability of the numerical integration. To examine the reliability, we have used the fact that only the normal modes of odd wave number are allowed when the initial excited mode has odd wave number; the spectra of the harmonic energy E_i have been examined at the ends of some runs. We confirmed that only the odd modes were excited, while energy of the even modes was sufficiently small and negligible. This supports the reliability of the numerical integration.

Figure 3 shows the inverse of the relaxation time $1/\tau_R$ plotted against k/N and ϵ. $1/\tau_R$ is represented in Fig. 3(a)

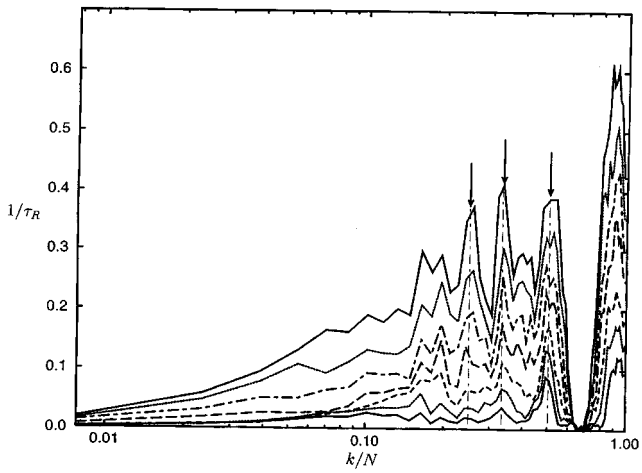

FIG. 4. Sectional curves of the $1/\tau_R$ at several different values of the energy density. From top to bottom $\epsilon=100, 50.2, 25.1, 12.6, 6.31, 2.52$, and 1.00.

and the contour plot is in Fig. 3(b). For a set of k/N and ϵ, we have made the numerical integration with two different initial conditions: one, that all energy is given in the kinetic part, i.e., $Q_k(0)=0, \frac{1}{2}\dot{Q}_k^2(0)=E$, and the other that all energy is given in the potential part, i.e., $\dot{Q}_k(0)=0, \frac{1}{2}\omega_k^2 Q_k^2(0)+(3\beta/8N)\omega_k^4 Q_k^4(0)=E$ [cf. Eq. (8)]. There was no significant difference between the relaxation times τ_R of both initial conditions and we evaluated the relaxation time τ_R by the average of those of the two initial conditions.

$1/\tau_R$ shown in Figs. 3(a) and 3(b) is quite similar to the LCE shown in Figs. 2(a) and 2(b). Interestingly, there is the interval in the wave number in which $1/\tau_R$ shows a sharp decrease and remains remarkably small even at the large energy density. The interval is found at $k/N\simeq 0.7$, which is the same as the value obtained by the LCE analysis. The existence of the interval is clearly shown in Fig. 4, which gives some sectional plots of $1/\tau_R$ at fixed values of ϵ. This experimental result is quite consistent with the prediction of the LCE analysis and gives strong evidence for the existence of the stability band.

The ridge structure can also be found in the wave-number range smaller than that of the stability band: some peaks of $1/\tau_R$ appear intermittently at some specific values of k/N. The ridge structure can be seen in Fig. 4, where the peaks of $1/\tau_R$ indicated by arrows appear at $k/N\simeq$ 0.50, 0.34, and 0.24. This feature is also in agreement with the prediction by the LCE. One may suspect that the peaks could be attributed to the statistical error. However, we conclude that the observed ridge structure is not due to the statistical error but the intrinsic structure, based on the fact that, in Fig. 4, the peaks appear at definite values of k/N that are predicted by the LCE analysis when ϵ is changed.

The decay curves of $\eta(t)$ of the modes of $k=85$, 65, and 51 are shown in Figs. 5(a), 5(b), and 5(c), respectively. The above modes correspond to three typical cases of stability: $k=85$ ($k/N\simeq 0.66$) and $k=65$ ($k/N\simeq 0.51$) correspond to the stability band and peak of $1/\tau_R$, respectively, and $k=51 (k/N\simeq 0.40)$ is chosen from the wave-number range that is neither the stability band nor the peak of $1/\tau_R$.

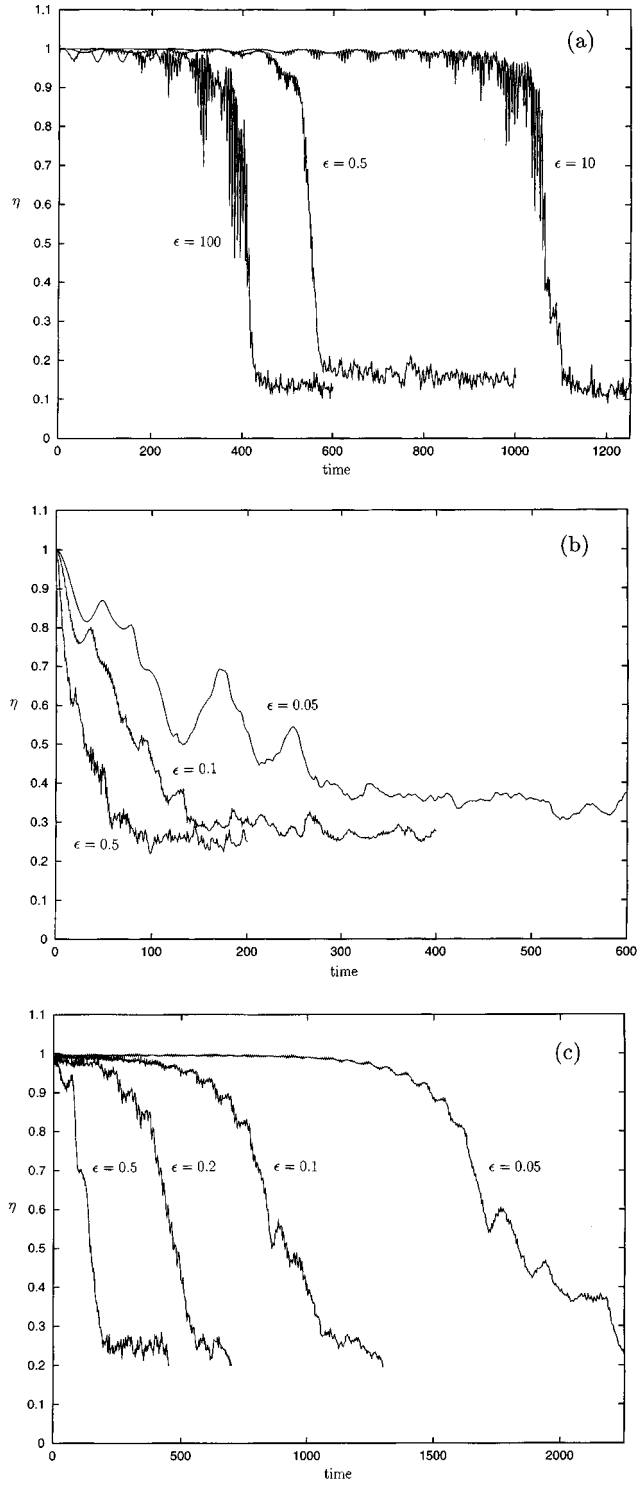

FIG. 5. Time evolution of $\eta(t)$. (a) $k=85$, (b) $k=65$, and (c) $k=51$.

The induction phenomenon [8,9] is clearly seen in all curves of $k=81$, in Fig. 5(a): $\eta(t)$ remains almost unity for a certain period, which is called the induction period, and then abruptly decreases. It should be noted that the induction phenomenon can still be observed even at the large energy density. By contrast, no induction period can be observed in the curves of $k=65$, in Fig. 5(b), though the energy densities are much smaller than those of the previous case. Since the stability of the mode of $k=51$ is intermediate between $k=85$ and 65, it is expected that the behavior of $\eta(t)$ is also an intermediate one. In fact, the induction phenomenon can be observed for the smaller energy density $\epsilon=$ 0.05, 0.10, and 0.20, while for the larger energy density $\epsilon=0.50$ it cannot be observed.

During the induction periods, the energy exchanges among the normal modes are weak and regular, which may be attributed to the motions stuck in thin stochastic layers of the deformed Kolmogorov-Arnold-Moser (KAM) tori. The abrupt decreases of $\eta(t)$ following the induction periods stand for the stochastic energy exchanges due to the diffusion towards the stochastic sea in phase space. Therefore, vanishing of the induction period can be considered to indicate the destruction of the KAM torus. In view of this, the above examples of $\eta(t)$ indicate that, for the modes within the stability band, the corresponding KAM tori are not destroyed but persist even at the large energy density, while for the modes corresponding to the peaks of $1/\tau_R$ the KAM tori are destroyed at sufficiently smaller energy density. That is, roughly speaking, larger $1/\tau_R$ means smaller energy density at which the destruction of the KAM torus occurs. Consequently, the destruction of the KAM tori that correspond to the single-mode oscillation proceeds quite inhomogeneously in phase space with an increase in the energy density: the energy density for the destruction is strongly dependent on the wave number of the normal mode, affected by the ridge structure or the stability band. We note that, in the smaller range of wave numbers (roughly $k/N<0.10$), the induction period vanishes at much smaller energy density than that expected from the small $1/\tau_R$ of those modes. In this range of wave numbers, the smallness of $1/\tau_R$ may be mainly due to the small characteristic frequency ω_k and does not mean the persistence of the KAM tori at the larger energy density.

The narrow packet excitation is physically more relevant than the single-mode excitation. Therefore, it should be examined whether the above-mentioned features, namely, the ridge structure and the stability band, are relevant for the narrow packet excitation. We have carried out only preliminary numerical experiment, where the narrow packet that consists of two normal modes with equal energy, an odd mode and next even mode, is excited as the initial condition. The features were clearly observed in the experimental results and then the relevance of the features for the narrow packet excitation was supported.

IV. CONCLUSION

The stability of the normal mode in short periods of time has been studied under the single-mode excitation condition, for the FPU-β model. The main purpose is to determine the stability against both the energy density and the excited mode's wave number. As probes for examining the stability the LCE of the average variational equation and the relaxation time τ_R were employed. The results obtained both by the LCE and by the relaxation time are in good agreement with each other.

The results show that the stability is intricately dependent on both the energy density and the excited mode's wave number. The results can be summarized as follows. (i)

Roughly speaking, the motion tends to be more stochastic for larger energy density and larger wave number. (ii) There is the interval for the particular stability in the wave number: the normal mode whose wave number is included in the interval is extremely stable, i.e., the stability band. The interval is located at $k/N \simeq 0.70$. (iii) The stochasticity is enhanced intermittently at some specific values of the wave number, i.e., the ridge structure. Feature (i) agrees with the well-known analytical results by Izrailev and Chirikov reported in Ref. [3]; however, the other two features (ii) and (iii) are quite different. The finding of these features is the main consequence of the present paper. The relevance of these features for the narrow packet excitation has been supported also by preliminary numerical experiments. In the present paper, our study was made for the FPU-β model, but similar features may be found in other one-dimensional anharmonic lattice models. The problem whether the observed features, the stability band or the ridge structure, can be observed even at the thermodynamic limit remains open to the future work. In addition to the results mentioned above, it also has been confirmed that the average variational equation approach is quite useful, which was proposed as a theoretical approach to examine the stability of the normal mode in short periods of time.

ACKNOWLEDGMENT

The author wishes to thank Professor T. Munakata for helpful suggestions.

[1] E. Fermi, J. Pasta, and S. Ulam, *Collected Papers of E. Fermi*, edited by E. Segre (University of Chicago, Chicago, 1965).
[2] N. J. Zabusky and M. D. Kruskal, Phys. Rev. Lett. **15**, 240 (1965).
[3] F. M. Izrailev and B. V. Chirikov, Dokl. Akad. Nauk SSSR **166**, 57 (1966) [Sov. Phys. Dokl. **11**, 30 (1966)].
[4] G. P. Berman and A. R. Kolovskij, Zh. Éksp. Teor. Fiz. **87**, 1938 (1984) [Sov. Phys. JETP **60**, 1116 (1984)].
[5] N. Budinsky and T. Bountis, Physica D **8**, 445 (1983).
[6] R. L. Bivins and N. Metropolis, J. Comput. Phys. **12**, 65 (1973).
[7] C. F. Driscoll and T. M. O'Neil, Phys. Rev. Lett. **37**, 69 (1976).
[8] N. Saito, N. Ooyama, Y. Aizawa, and H. Hirooka, Prog. Theor. Phys. Suppl. **45**, 209 (1970).
[9] N. Saito, N. Hirotomi, and A. Ichihara, J. Phys. Soc. Jpn. **39**, 1431 (1975).
[10] P. Bocchieri, A. Scotti, B. Bearzi, and A. Loinger, Phys. Rev. A **2**, 2013 (1970).
[11] M. Pettini and M. Landolfi, Phys. Rev. A **41**, 768 (1990).
[12] M. Pettini and M. Cerruti-Sola, Phys. Rev. A **44**, 975 (1991).
[13] M. Pettini, Phys. Rev. E **47**, 828 (1993).
[14] L. Casetti and M. Pettini, Phys. Rev. E **48**, 4320 (1993).
[15] L. Casetti, R. Livi, and M. Pettini, Phys. Rev. Lett. **74**, 375 (1995).
[16] H. Kantz, Physica D **39**, 322 (1989).
[17] G. M. Zaslawsky, *Chaos in Dynamic System* (Harwood Academic, Amsterdam, 1987).